Phase Calibration Tone Processing With the Block II VLBI Correlator

C. S. Jacobs[1]

A review of phase calibration tone processing is given as it applies to a typical radio reference frame experiment processed with the Block II very long baseline interferometry (VLBI) correlator. Because much of the Block II correlator processing is similar to that of the Block 0's, our discussion largely follows Thomas's [4] discussion of Block 0 phase calibration processing. The Block II's 127-level tone model is the most significant change from the Block 0's tone processing. We discuss the definitions of the quantities in the Block II output file in sufficient detail to allow the calculation of tone amplitude, phase, and their respective variances. After reviewing the assumptions and approximations made in tone processing, we conclude that the tone amplitude variance is a function of one parameter—the number of bits correlated—to within ±10. This 10 percent uncertainty is due to oversampling, finite side-band rejection, clipper bias, and phase model quantization. Each of these effects is examined theoretically and experimentally and is shown to affect tone amplitude variance by less than 10 percent.

I. Introduction

The instrumentation used to collect very long baseline interferometry (VLBI) data introduces phase shifts that corrupt the estimated phase and group delay of the incoming quasar or spacecraft signal. In order to calibrate these instrumental phase shifts, a technique known as phase calibration has been developed [1,3].[2] The phase calibration system compensates for instrumental phase errors by generating a signal of known phase, inserting this signal into the VLBI instrumentation, and examining the signal's phase after it has traversed the instrumentation. This calibration signal is embedded as a set of low-level monochromatic signals ("tones") in the broadband VLBI data stream. Typically the calibration signal power is less than 1 percent of the broadband VLBI signal. These tones are extracted in post-real time from the VLBI data stream by customized signal-processing hardware called the correlator.

The present discussion will focus on phase calibration extraction as implemented in the Block II correlator[3,4] [5] and subsequent processing. Section II will discuss 1-bit sampling, its effects on amplitude

[1] Tracking Systems and Applications Section.

[2] J. L. Fanselow, "The Use of a Phase Calibrator in VLBI to Remove Receiving System Phase Shifts," JPL Interoffice Memorandum 315.2.011 (internal document), Jet Propulsion Laboratory, Pasadena, California, October 1976.

[3] E. H. Sigman, "Phase Cal Board," unpublished (internal document), Jet Propulsion Laboratory, Pasadena, California, April 21, 1986.

[4] T. O'Connor, *Introduction to Block II VLBI Correlator Hardware*, JPL manual (internal document), Jet Propulsion Laboratory, Pasadena, California, April 1, 1989.

scale, and the assumption that three-tone intermodulation products are small. Section III will review the "tone stopping" procedure used by the correlator to extract the tone signal from the sampled data. Section IV gives an expression for tone variance, examines the assumption that the sampled bits have a small DC bias, and shows that the correlation between bits contributes to the tone variance. Section V discusses our method for calculating the digital autocorrelation for the sampled bit stream. Results are given for three slightly oversampled bandpasses: square, 11-pole Butterworth (Mk II), and 7-pole Butterworth (Mk III). Section VI examines the variation in digital autocorrelation versus tone frequency for our typical Mk III configuration. Section VII gives our final expressions for tone amplitude and phase variance in light of the preceding discussion. Section VIII summarizes the article. Appendices A through D give detailed results of theoretical digital autocorrelation, Mk II empirical autocorrelation, Mk III empirical autocorrelation, and an examination of our assumption that finite side-band rejection has a small effect on tone variance, respectively.

This article will show that effects due to correlator phase model quantization, sampler DC bias, side-band rejection, and autocorrelation (from oversampling) are all negligible. In particular, the effects of model quantization and DC bias have been reduced in the Mk III system as compared with the Mk II system and now contribute less than 1 percent of the total variance. The largest effect, autocorrelation, alters tone variance by 9 percent or less and varies slightly as a function of baseband tone frequency. As a result, to within 10 percent, the variance of the stopped-tone voltage, σ_V^2, is just the inverse of the number of bits per measurement, N_t, with a scale factor of 1/2 to account for the average of the sinusoidal stopping function:

$$\sigma_V^2 = \frac{1}{2N_t} \tag{1}$$

The voltage signal-to-noise ratio is given by $SNR_V = \sqrt{C^2 + S^2}/\sigma_V$, where C and S are the "rezeroed" (debiased), normalized cosine and sine counts from the correlator. For $SNR_V > 10$, the variance in the tone phase is just $1/SNR_V^2$,

$$\sigma_\phi^2 = \frac{1}{2N_t\left[C^2 + S^2\right]} \tag{2}$$

Unless otherwise stated, our "typical" Mk III configuration assumes the following configuration:

(1) Mk III recording mode C: 14 upper side-band channels

(2) 7-pole Butterworth filter with a cutoff frequency $\nu_0 = 1.8$ MHz

(3) 4 Mbit sec^{-1} sample rate per channel

(4) Phase calibration tones spaced every 0.5 MHz

(5) Nominal baseband frequencies of 0.24, 0.74, 1.24, and 1.74 MHz

(6) Block II phase model quantized to 256 levels in argument and 127 levels in amplitude

II. Data Quantization

In the Mk II and Mk III VLBI systems, the signal is 1-bit sampled. This makes near-optimal best use of the available recorded bandwidth. Although digitally formatted data have advantages for subsequent processing, there are some "side-effects" to be aware of, namely, amplitude scale changes and the creation of intermodulation products. To see this, we start with Thomas's [4] Eq. (F8),

$$\left\langle \tilde{V} \right\rangle = \int_{-\infty}^{\infty} Q(V)\ P(V)\ dV \tag{3}$$

where V is the analog voltage, $< >$ indicates an ensemble average, $\tilde{V}$ indicates a 1-bit quantized voltage, $P(V)$ is the probability distribution of the voltage, and $Q(V)$ is the sampling function. From Sigman, the two kinds of bits that enter the Block II are treated as ± 1 by the phase calibration extractor (despite tendencies to call them 0's and 1's).[5] Thus,

$$Q(V) = +1, \quad V > 0 \tag{4}$$

$$= -1, \quad V < 0 \tag{5}$$

Following Thomas's Eqs. (F1) and (F2) [4], we will define a signal, S, as the sum of n tones (typically equally spaced in frequency):

$$S = \sum_n v_n \cos(\phi_n) \tag{6}$$

where v_n and ϕ_n are the amplitude and phase of the nth harmonic of the phase calibration pulse. Assuming Gaussian noise of variance, σ^2, about the signal voltage, S,

$$P(V) = \frac{1}{\sqrt{2\pi}\sigma} \exp\left[\frac{(V-S)^2}{2\sigma^2}\right] \tag{7}$$

Making a change of variable to $z = (V-S)/\sqrt{2}\sigma$, we have

$$\left\langle \tilde{V} \right\rangle = \frac{1}{\sqrt{\pi}} \int_{-\infty}^{\infty} Q(S + \sqrt{2}\sigma z) e^{-z^2}\ dz \tag{8}$$

And the sampling function, Q, is now

$$Q(S + \sqrt{2}\sigma z) = +1, \quad z > \frac{-S}{\sqrt{2}\sigma} \tag{9}$$

$$= -1, \quad z < \frac{-S}{\sqrt{2}\sigma} \tag{10}$$

Noting that e^{-z^2} is an even function and that the integral from $-\infty$ to ∞ of a normalized Gaussian is unity, we arrive at

$$\left\langle \tilde{V} \right\rangle = \frac{2}{\sqrt{\pi}} \int_0^{S/\sqrt{2}\sigma} e^{-z^2} dz \tag{11}$$

[5] E. H. Sigman, op. cit., Section 1.4.

Following Sigman,[6] the exponential can be expressed as a power series,

$$e^{-z^2} = \sum_k (-1)^k \frac{z^{2k}}{k!} \tag{12}$$

The integral then is straightforward:

$$\left\langle \tilde{V} \right\rangle = \frac{2}{\sqrt{\pi}} \sum_{k=0}^{\infty} \frac{(-1)^k \left(\frac{S}{\sqrt{2}\sigma} \right)^{2k+1}}{k!\ (2k+1)} \tag{13}$$

Thus, the 1-bit quantization process produces a series of terms that are odd powers of the analog signal. Assuming that $S << \sqrt{2}\sigma$, we need only to retain the first few terms of the series:

$$\left\langle \tilde{V} \right\rangle = \sqrt{\frac{2}{\pi}} \left[\frac{S}{\sigma} - \frac{1}{6} \left[\frac{S}{\sigma} \right]^3 + \cdots \right] \tag{14}$$

The scale factor ($\sqrt{2/\pi}$) introduced in the digital signal processing has now become apparent. Also, the intermodulation products are now manifest in the S^3 term in Eq. (14). These products are sums of all combinations of three tones beating against each other and are of the form

$$S^3 = \sum_{l,m,n} v_l\ v_n\ v_m \cos(\phi_l) \cos(\phi_m) \cos(\phi_n) \tag{15}$$

In the Mk III VLBI system, the video-converter baseband filter effectively limits the sums over l, m, and n to just the tones within the baseband frequency range. As a result, the sums typically will cover two to four tones rather than all the tones over the full radio-frequency range (e.g., for 0.5-MHz tone spacing, there are 800 tones over the full X-band range of 8200 to 8600 MHz).

Our typical Mk III VLBI experiment uses four tones per baseband channel, which are placed at 0.5-MHz intervals. The tone generator output is adjusted so that each tone has ≈0.36 percent rms power per tone relative to the noise power in the 2-MHz-wide channel. The rms power per tone can be expressed in terms of variables that we have defined as

$$P_{rms} = \frac{1}{2} \left[\frac{v_n}{\sigma} \right]^2 \tag{16}$$

This gives a typical analog voltage SNR for a single tone of

$$\frac{v_n}{\sigma} = 0.085 \tag{17}$$

From Eq. (14), we see that the three-tone intermodulation products are a factor of $(1/6)(S/\sigma)^2$ smaller than the desired signal. Thus, for typical signal levels, three-tone products will be ≈0.001 times the

[6] E. H. Sigman, "Phase Measurement of Sinusoid Tones Buried in Noise," JPL Engineering Memorandum 315-74 (internal document), Jet Propulsion Laboratory, Pasadena, California, November 21, 1978.

desired signal. As long as the sums in Eq. (15) are limited to just a few tones by the baseband filters, the sum of these small third-order intermodulation products should contribute less than 1 percent to Eq. (14). Therefore, we will neglect third-order intermodulation products from this point on.

III. Tone Stopping

Because the SNR per bit of a given tone is <<1, in order to detect a tone the correlator must average over many bits (gaining SNR as $\sqrt{N_t}$, where N_t is the number of bits). However, the tones are recorded at baseband frequencies that typically are from 0 to 2 MHz, having been sampled at 4 Mbit $\sec^{-1}$. At these frequencies, a sinusoidal signal will start averaging toward zero on a time scale of μs (a few bits). To overcome this problem, the correlator digitally heterodynes the tones from their baseband frequency to near DC. This procedure is known as "tone stopping." The stopped voltage of tone n, $\left\langle \tilde{V}_n \right\rangle$, is expressed as follows:

$$\left\langle \tilde{V}_n \right\rangle = \frac{1}{N_t} \sum_{k=1}^{N_t} \tilde{V}_k e^{i\psi_{nk}} \tag{18}$$

where the index k represents the kth sample or bit, the index n indicates the nth tone [cf., Eq. (6)], and ψ_{nk} is the model phase for tone n at sample time k.

A. Phase Model Quantization

Because tone stopping is calculated using digital circuitry in the correlator, the quantities in Eq. (18) must be quantized. This inevitably requires design trade-offs that balance requirements for speed and cost versus accuracy. In the Block II correlator, this balance point was set with the phase argument, ψ_{nk}, quantized to 256 levels and the amplitude to 127 levels. The deviation of this quantized model from the ideal has small discontinuous steps or "sharp edges" that may be represented by higher-order harmonics of the desired function, $e^{i\psi}$. A Fourier transform of the quantized function shows that almost all the power is in the fundamental and very little power goes into the higher harmonics. Table 1 compares the three largest terms for Fourier series representing (1) a square wave, (2) the three-level Block 0 stopping function, and (3) the Block II 127-level stopping function.

Table 1. Phase quantization effects.

No. of levels	Harmonic number	Fourier coefficient
2	1	+1.2732
	3	+0.4244
	5	+0.2547
3	1	+1.1763
	3	+0.1624
	5	−0.0975
127	1	+1.0012
	3	+0.0005
	5	−0.0006
	255	−0.0039
	257	−0.0039

The old Block 0 stopping function introduces a scale factor of 1.18 and has a large and undesired third harmonic that can correlate with three-tone products in the digital signal [cf., Eq. (15)]. In comparison, the Block II stopping function is very close to ideal. The first harmonic's coefficient of 1.001 is so close to unity that we will ignore the difference. The Block II's largest harmonics (the 255th and 257th) are caused by beating of the fundamental with the 256-level quantization; their amplitudes are a factor $1/256$ smaller than the fundamental. The largest undesired terms in the Block II are a factor of 40 smaller than in the Block 0. We especially note that the potentially troublesome third harmonic is down at 5×10^{-4}. As a result, we will consider Block II phase-model quantization effects to be negligible in further discussions.

B. Heterodyning

The Block II correlator implements the $e^{i\psi_{nk}}$ stopping function of Eq. (18) by breaking it into cosine and sine components—with separate circuitry for each component. We will denote these separate components as the real and imaginary parts of the equations that follow:

$$\left\langle \tilde{V}_n \right\rangle = \frac{1}{N_t} \sum_{k=1}^{N_t} \tilde{V}_{kn} \left[\cos(\psi_{nk}) + i \sin(\psi_{nk}) \right] \tag{19}$$

C. Stopping Function Bias and Scale

In the actual Block II hardware, there is one further complication. The stopping functions as implemented have a DC bias and a scale factor:

$$\cos(\psi_{nk}) \rightarrow 64 + 63 \cos(\psi_{nk}) \tag{20}$$

$$\sin(\psi_{nk}) \rightarrow 64 + 63 \sin(\psi_{nk}) \tag{21}$$

The bias was chosen so that the stopping function is never negative. Freed from the need to decrement to obtain intermediate results in the sum, the hardware implementation can use just a simple accumulator. Because of this, Eq. (19) actually is implemented in hardware as

$$\left\langle \tilde{V}_n \right\rangle = \frac{1}{N_t} \sum_{k=1}^{N_t} 64(1+i) + \tilde{V}_{kn} 63 \left[\cos(\psi_{nk}) + i \sin(\psi_{nk}) \right] \tag{22}$$

Ignoring the third-order intermodulation products [cf., Eqs. (14) and (15)], the data signal is

$$\tilde{V}_{kn} = \left[\frac{1}{\sqrt{2\pi}} \frac{v_n}{\sigma} \right] \cos(\phi_{nk}) \tag{23}$$

Substituting this into Eq. (19), we will have terms of the form

$$\cos(\phi_n) \cos(\psi_n) = \frac{1}{2} \left[\cos(\phi_n + \psi_n) + \cos(\phi_n - \psi_n) \right] \tag{24}$$

$$\cos(\phi_n) \sin(\psi_n) = \frac{1}{2} \left[\sin(\phi_n + \psi_n) - \sin(\phi_n - \psi_n) \right] \tag{25}$$

The $(\phi_n - \psi_n)$ terms are what we call the stopped tone. Given that $\phi_{nk} - \psi_{nk} \approx 0$, these terms have nearly zero frequency—hence the term "stopped." The $(\phi_n + \psi_n)$ terms will average to nearly zero since they oscillate at twice the tone's baseband frequency, which typically is in the range of megahertz, causing them to average out on a time scale of μs. The correlator sends its output from the sums *before* averaging, i.e., the $1/N_t$ averaging factor is not applied by the correlator. Furthermore, the hardware applies a scale factor of 1/256 to its output.[7] This occurs because the Block II has a two-step procedure to produce cosine and sine counts. First, it adds up the results of the data times the phase model,

$$\sum_{k=1}^{N_t} 64(1+i) + \tilde{V}_{kn} 63 \left[\cos(\psi_{nk}) + i \sin(\psi_{nk})\right] \tag{26}$$

in an 8-bit accumulator. Second, the accumulator is followed by a 16-bit counter that increments every time the eighth bit of the accumulator rolls over. Thus, the counter is incremented only once for every 2^8 (= 256) "accumulations" recorded by the accumulator. Labeling the real and imaginary components of $\left\langle \tilde{V}_n \right\rangle$ as they are output from the correlator as $\hat{C}$ and $\hat{S}$, respectively,

$$\hat{C} = \frac{N_t}{256}\left[64 + 63\left[\frac{1}{\sqrt{2\pi}}\frac{v_n}{\sigma}\right]\langle\cos(\phi_n - \psi_n)\rangle\right] \tag{27}$$

$$\hat{S} = \frac{-N_t}{256}\left[64 + 63\left[\frac{1}{\sqrt{2\pi}}\frac{v_n}{\sigma}\right]\langle\sin(\phi_n - \psi_n)\rangle\right] \tag{28}$$

The quantity N_t is not available directly from the correlator output. The correlator only reports (1) N_d, the total number of bits per integration period and (2) $\hat{I}$, half the number of invalidated bits per integration. The N_d is divided by four to account for the four-way time multiplexing of the tone extractor hardware, i.e., only one in four bits is processed for any given tone:

$$N_t = \frac{N_d}{4} - 2\hat{I} \tag{29}$$

The post-correlation software then must remove the bias and correct for the scale factors in order to extract the desired tone amplitude and phase. The following two equations relate the correlator output quantities, $\hat{C}$ and $\hat{S}$, to the debiased and normalized quantities, C and S, respectively:

$$C = \left[\frac{1}{\sqrt{2\pi}}\frac{v_n}{\sigma}\right]\cos(\phi_n - \psi_n) = \frac{4\hat{C} - N_t}{\left(\frac{63}{64}\right)N_t} \tag{30}$$

$$S = \left[\frac{1}{\sqrt{2\pi}}\frac{v_n}{\sigma}\right]\sin(\phi_n - \psi_n) = \frac{4\hat{S} - N_t}{\left(\frac{63}{64}\right)N_t} \tag{31}$$

We note that some utility programs simplify the above two equations by setting 63/64 = 1, thereby slightly distorting the amplitude without harming the phase.

[7] E. H. Sigman, 1986, op. cit., Section 1.6.

From Eqs. (30) and (31), it is easy to calculate the amplitude and residual phase for the *digitized* and *stopped* tone:

$$|\tilde{V}_n| = \frac{1}{\sqrt{2\pi}} \frac{v_n}{\sigma} = \sqrt{C^2 + S^2} \tag{32}$$

$$\langle \phi_n - \psi_n \rangle = -\arctan \frac{S}{C} \tag{33}$$

The origin of the minus sign in Eq. (33) may be seen more clearly by examining Eq. (25). The phase in Eq. (33) is an average residual phase in the sense that we have averaged over N_t bits and taken the residual relative to the model phase ψ_n.

IV. Tone Variance

Having reviewed the basic signal processing done on phase calibration tones by the Block II correlator, we will now examine in some detail the variance of the tone amplitude. We will discuss the various approximations and assumptions that are made in the Block II as they affect the tone variance.

Using the notation of Thomas's Eq. (F20) [4], the stopped-tone variance is

$$\sigma_V^2 = \frac{1}{N_t^2} \sum_k^{N_t} \sum_l^{N_t} \left[\left\langle \tilde{V}_k \tilde{V}_l \right\rangle - \left\langle \tilde{V}_k \right\rangle \left\langle \tilde{V}_l \right\rangle \right] \cos(\psi_{nk}) \cos(\psi_{nl}) \tag{34}$$

Following the convention given in Eqs. (4) and (5) (also, cf., Sigman[8]), the quantized voltage for the kth voltage sample is

$$\tilde{V}_k = +1 \quad \text{if } V > 0 \tag{35}$$

$$\tilde{V}_k = -1 \quad \text{if } V < 0 \tag{36}$$

We first will consider the terms of Eq. (34) for which $k = l$ and then consider the terms for which $k \neq l$.

Since $\tilde{V}_k = +1$ or -1, we have

$$\left\langle \tilde{V}_k^2 \right\rangle = 1 \tag{37}$$

Thus,

$$\sum_k^{N_t} \sum_{l=k} \left\langle \tilde{V}_k^2 \right\rangle = N_t \tag{38}$$

[8] Ibid.

Next we consider terms of the form $< \tilde{V}_k >$. Since the voltage should have no DC component, the ensemble average voltage should be zero, $< \tilde{V}_k >= 0$. In practice, the clipper circuit that quantizes the data is susceptible to small voltage biases. This causes the data to have an excess of "1" bits or "0" bits, resulting in a nonzero ensemble average for $\tilde{V}_k$, which we will call the DC bias. Taking the excess number of "1" bits, n_1, compared with the number of "0" bits, n_0, and normalizing by the total number of bits, we obtain the DC bias from the ensemble average for $\tilde{V}_k$,

$$\left\langle \tilde{V}_k \right\rangle = \left\langle \frac{n_1 - n_0}{n_1 + n_0} \right\rangle \tag{39}$$

An examination of 10 scans from each of two experiments, 89ca127 (DSS 14 and DSS 43) and 90cs054 (DSS 15 and DSS 65), both of which were recorded using Mk III mode C, shows that typical DC biases range from 5×10^{-4} to 5×10^{-3} with an occasional channel as high as 0.01 to 0.02. By comparison, Young measured fractional DC biases for the Mk II system of 0.002 to 0.05.[9]

Taking a DC bias of 10^{-3} to be representative of a "good" Mk III clipper and 10^{-2} a "bad" Mk III clipper,

$$\left\langle \tilde{V}_k \right\rangle \left\langle \tilde{V}_k \right\rangle = 10^{-6} \text{ to } 10^{-4} \tag{40}$$

We will neglect this as compared with the unity term, $< \tilde{V}_k^2 >$, from Eq. (34). Noting that $\left\langle \cos^2(\psi_{nk}) \right\rangle = 1/2$, one has

$$\sigma^2(k = l) = \frac{1}{N_t^2} \sum_{k}^{N_t} 1 \times \cos^2(\psi_{nk}) \tag{41}$$

$$\sigma^2(k = l) = \frac{1}{2N_t} \tag{42}$$

Next we consider the terms for which $k \neq l$:

$$\sigma_V^2(k \neq l) = \frac{1}{N_t^2} \sum_{k}^{N_t} \sum_{l \neq k}^{N_t} \left[\left\langle \tilde{V}_k \tilde{V}_l \right\rangle - \left\langle \tilde{V}_k \right\rangle \left\langle \tilde{V}_l \right\rangle \right] \cos(\psi_{nk}) \cos(\psi_{nl}) \tag{43}$$

The $< \tilde{V}_k \tilde{V}_l >$ term is a measure of the correlation between bits and is ≈10 percent for typical VLBI systems. This autocorrelation term is discussed in detail in Section V, which follows. As shown in Eq. (40), the $< \tilde{V}_k >< \tilde{V}_l >$ term is of order 10^{-4} to 10^{-6} and will be considered negligible for our present purposes. The product of the cosines can be expressed as the usual sum and difference of frequencies:

$$\cos(\psi_{nk}) \cos(\psi_{nl}) = \frac{1}{2} \left[\cos(\psi_{nk} - \psi_{nl}) + \cos(\psi_{nk} + \psi_{nl}) \right] \tag{44}$$

[9] L. E. Young, "The Placement of Phase Calibrator Tones," JPL Interoffice Memorandum 315.2-96 (internal document), Jet Propulsion Laboratory, Pasadena, California, May 9, 1979.

The second term, because of its high frequency, will average out when summed over many bits (typically N_t is of order 10^6). While extracting spacecraft tones may require a phase model, ψ_{nk}, with second-order or higher terms, for extracting phase calibration tones, a linear phase model usually is sufficient. Thus,

$$\psi_{nk} - \psi_{nl} = \omega_n(t_k - t_l) \tag{45}$$

where ω_n is the radian frequency of tone n and t_k is the time at which the kth voltage sample, $\tilde{V}_k$, was taken. Thus, the $k \neq l$ terms simplify to

$$\sigma_V^2(k \neq l) = \frac{1}{N_t^2} \sum_{k}^{N_t} \sum_{l \neq k}^{N_t} \left\langle \tilde{V}_k \tilde{V}_l \right\rangle \frac{1}{2} \cos(\omega_n(t_k - t_l)) \tag{46}$$

In summary, we started with an expression for the tone variance, Eq. (34). We have shown that, if one may assume that (1) the DC biases [Eq. (39)] are small and (2) the autocorrelations between bits, [Eq. (46)], are small, then the tone variance depends only on the number of bits in a sample, N_t. We gave some evidence that the first assumption is a good one. We will now proceed in the next two sections to examine the second assumption that the autocorrelation is negligible.

V. Digital Autocorrelation

The digital autocorrelation is a measure of the statistical independence of the voltage samples, $\tilde{V}_k$. In order to calculate the digital autocorrelation, we will make use of relations between (1) digital and analog autocorrelation, (2) analog autocorrelation and analog power spectrum, and (3) sample rate and bandwidth. First we will define the digital autocorrelation, $\tilde{R}(\tau)$, as

$$\tilde{R}(\tau) = \left\langle \tilde{V}_k \tilde{V}_l \right\rangle \tag{47}$$

where $\tau = t_k - t_l$ is the time offset between the quantized voltage samples $\tilde{V}_k$ and $\tilde{V}_l$.

A. Relation Between Digital and Analog Autocorrelation

The digital autocorrelation, $\tilde{R}(\tau)$, may be determined from the analog autocorrelation, $R(\tau)$, according to the van Vleck relation [6]:

$$\tilde{R}(\tau) = \frac{2}{\pi} \sin^{-1}(R(\tau)) \tag{48}$$

Assuming that $R(\tau) << 1$, one may make the approximation $\sin^{-1}(R(\tau)) \approx R(\tau)$, thereby simplifying the above relation to

$$\tilde{R}(\tau) = \frac{2}{\pi} R(\tau) \tag{49}$$

Noting that $k \neq l$ is equivalent to $\tau \neq 0$, and $\sum_k^{N_t} \sum_{k \neq l} = N_t \sum_{k \neq l}$, we have the second term of Thomas's Eq. (F21) [4]:

$$\sigma_V^2(k \neq l) = \frac{1}{2N_t} \sum_{\tau \neq 0} \frac{2}{\pi} R(\tau) \cos(\omega_n \tau) \tag{50}$$

Given this approximation and ignoring DC biases, we now can express the tone variance from Eq. (34) as a function of the number of bits, N_t, and the *analog* autocorrelation, $R(\tau)$:

$$\sigma_V^2 = \frac{1}{2N_t} \left[1 + \frac{2}{\pi} \sum_{\tau \neq 0} R(\tau) \cos(\omega_n \tau) \right] \tag{51}$$

This shows that the tone variance depends mainly on the number of bits in a given sum with a small correction to account for the correlation between sampled bits. We will now show that the correlation between bits is only a few percent and depends on bandpass shape, sample rate, and tone frequency.

B. Calculating the Autocorrelation From the Power Spectrum

In order to calculate the analog autocorrelation, $R(\tau)$, we make use of the Wiener–Khinchin relation, which states that the autocorrelation is equal to the Fourier transform of the amplitude power spectrum, $A(\nu)$. Ignoring normalization factors for the moment, the autocorrelation can be expressed as

$$R(\tau) = \int_0^\infty d\nu \cos(2\pi\nu\tau) A(\nu) \tag{52}$$

Since the recorded signal is real, the above expression uses a cosine transform rather than a complex transform. The normalization is implicitly determined when the Block II's phase calibration processing interprets bits as ± 1. This convention normalizes the *digital* autocorrelation at zero delay to unity [cf., Eq. (37)],

$$\tilde{R}(\tau = 0) = \left\langle \tilde{V}_k^2 \right\rangle = 1 \tag{53}$$

In order to obtain a consistent normalization for the analog autocorrelation, we insert a scale factor of $\pi/2$ and divide by the integral of the amplitude power spectrum, $A(\nu)$, to get

$$R(\tau) = \frac{\pi}{2} \frac{\int_0^\infty d\nu \cos(2\pi\nu\tau) A(\nu)}{\int_0^\infty d\nu A(\nu)} \tag{54}$$

In order to gain some insight into Eq. (54), we first will consider two idealized cases and then a third more realistic case: (1) an ideal square bandpass Nyquist sampled, (2) an ideal square bandpass slightly oversampled, and (3) a Butterworth bandpass slightly oversampled.

1. Case 1—Ideal Square Bandpass. If the power spectrum, $A(\nu)$, is a square bandpass of width ν_0, then

$$A(\nu) = \frac{1}{\nu_0} \quad \text{for } 0 \leq \nu \leq \nu_0 \tag{55}$$

$$= 0 \quad \text{elsewhere} \tag{56}$$

The autocorrelation then is a sinc function ($\mathrm{sinc}(x) = \sin(\pi x)/\pi x$),

$$R(\tau) = \frac{\pi}{2}\frac{\sin(2\pi\nu_0\tau)}{2\pi\nu_0\tau} \tag{57}$$

We have normalized so that the digital autocorrelation for $\tau = 0$ will be unity, $\tilde{R}(\tau=0)=(2/\pi)R(\tau=0) = 1$.

If samples are taken at the Nyquist sample rate, then the interval between bits will be

$$\tau_0 = \frac{1}{2}\nu_0 \tag{58}$$

For $\tau = k\tau_0$, i.e., integer bits (k is an integer $\neq 0$), the autocorrelation is zero:

$$R(k\tau_0)_{k\neq 0} = 0 \tag{59}$$

In other words, each bit is statistically independent of all other bits. Typical VLBI systems only approximate this ideal. Both the Mk II and Mk III VLBI systems' sample rates are slightly higher than the Nyquist rate, causing $R(k\tau_0)_{k\neq 0}$ to become nonzero.

2. Case 2—Oversampled Square Filter. If, instead of sampling at the Nyquist rate, we were to sample at a slightly higher frequency, $\nu_s > 2\nu_0$, then the autocorrelation at integer multiples of the bit spacing, $k\tau_0 = k/\nu_s$, would be

$$R(k\tau_0)_{k\neq 0} = \frac{\pi}{2}\frac{\sin\left(2\pi k\left(\frac{\nu_0}{\nu_s}\right)\right)}{2\pi k\left(\frac{\nu_0}{\nu_s}\right)} \tag{60}$$

The Mk II and Mk III systems can be approximated by a square filter with

$$\frac{2\nu_0}{\nu_s} \approx 0.9 \tag{61}$$

In this approximation, the autocorrelation is

$$R(k\tau_0)_{k\neq 0} = \frac{\pi}{2}\frac{\sin(0.9k\pi)}{0.9k\pi} \tag{62}$$

Again we use a normalization of $\pi/2$ so that $\tilde{R}(\tau = 0) = 1$. Figure A-1 in Appendix A gives plots of $\tilde{R}$ versus τ.

3. Case 3—Butterworth Lowpass Filter. A more accurate approximation of the Mk II and Mk III systems is obtained by assuming that the power spectrum of a given channel is described by the amplitude response of the baseband lowpass filter. Both the Mk II and Mk III VLBI systems use a Butterworth design for their baseband filters. The amplitude (power) response of a Butterworth filter as a function of baseband frequency, ν, and number of poles, n_p, is (e.g., [7])

$$A(\nu) = \frac{1}{1 + \left(\frac{\nu}{\nu_0}\right)^{2n_p}} \tag{63}$$

The Mk II typically uses $n_p = 11$ or $n_p = 13$, whereas the Mk III uses $n_p = 7$. For both the Mk II and the Mk III, the cutoff frequency is $\nu_0 \simeq 1.8$ MHz. Thus, for a Butterworth filter, the analog autocorrelation can be expressed as a function of τ, ν_0, and n_p:

$$R(\tau) = \frac{\pi}{2} \frac{\int_0^\infty d\nu \cos(2\pi\nu\tau) \left[1 + \left(\frac{\nu}{\nu_0}\right)^{2n_p}\right]^{-1}}{\int_0^\infty d\nu \left[1 + \left(\frac{\nu}{\nu_0}\right)^{2n_p}\right]^{-1}} \tag{64}$$

Because the autocorrelation decreases rapidly as $|\tau|$ increases, in practice we need only to calculate it for $\approx \pm 20$ bits or less. For the Mk II and Mk III, the sample rate usually is $\nu_s = 4$ Mbits/s, which makes τ equal to integer multiples of 0.25 μs.

With these parameters and scaling Eq. (64) by $2/\pi$ to convert the analog autocorrelation to digital, we have calculated the digital autocorrelation, $\tilde{R}(\tau)$. The results are in Table A-1 of Appendix A. Appendix A also contains Fig. A-1, which shows the digital autocorrelation for three different filters: (1) square bandpass, (2) Mk II: 11-pole Butterworth, and (3) Mk III: 7-pole Butterworth. All three filters have a cutoff frequency of $\nu_0 = 1.8$ MHz and a sample rate of $\nu_s = 4$ MHz that slightly oversamples the filtered signal.

Using the Block II correlator, the digital autocorrelation has been empirically determined for both Mk II and Mk III data. The Mk II results are presented in Appendix B and the Mk III results in Appendix C. Both Mk II and Mk III data show general agreement with the theory that we have presented. However, close quantitative agreement cannot be achieved without knowing the filter cutoff frequencies to about 1 percent. The results suggest that our nominal model with $\nu_0 = 1.8$ MHz may be in error by as much as 5 percent.

VI. Tone Variance Due to Mk III Autocorrelation

For the Mk II and Mk III systems that we have described, the contribution to the tone variance σ_V^2 due to autocorrelation of the bit stream typically is a few percent of σ_V^2. Consider our "typical" Mk III configuration: a 7-pole Butterworth filter with cutoff frequency $\nu_0 = 1.8$ MHz sampled at 4 Mbit s^{-1} with four tones placed at 0.24, 0.74, 1.24, and 1.74 MHz. These frequencies are 0.01 MHz below the nominal centers of the four Block II frequency "bins." The theoretical correction to the variance due to autocorrelation for these four tones is given in Table 2. The right-hand column in the table gives the fractional contribution to σ_V^2 due to autocorrelation. For experiments with slightly different frequencies, we note that the fractional contribution $(2N_t\sigma_V^2(k \neq l))$ varies by a few parts in 10^{-3} if ν_i is varied by 10 kHz. In summary, the autocorrelation needs to be considered only if one desires to calculate σ_V^2 to an accuracy of better than 10 percent. If one desires 1 percent accuracy, side-band rejection also should be considered. Side-band rejection is discussed further in Appendix D.

Table 2. Autocorrelation's contribution to tone variance.

Frequency, MHz	$2N_t\sigma_V^2(k \neq l)$
$\nu_1 = 0.24$	$+0.09$
$\nu_2 = 0.74$	$+0.04$
$\nu_3 = 1.24$	-0.04
$\nu_4 = 1.74$	-0.09

VII. Calculating Tone Variance

Having shown—both on theoretical and experimental grounds—that to within 10 percent the tone variance is just a function of the number of sampled bits, we now are ready to calculate the tone variance from the quantities output by the Block II correlator. From Eq. (42) we have, to ≈10 percent accuracy, the variance of the digitized and stopped-tone amplitude:

$$\sigma_V^2 = \frac{1}{2N_t} \tag{65}$$

The tone amplitude was defined in Eq. (32) as

$$\left|\left\langle \tilde{V}_n \right\rangle\right| = \frac{1}{\sqrt{2\pi}}\frac{v_n}{\sigma} = \sqrt{C^2 + S^2} \tag{66}$$

From this we obtain the stopped-tone *voltage* signal-to-noise ratio

$$SNR_V = \frac{\left\langle \tilde{V}_n \right\rangle}{\sigma_V} \tag{67}$$

$$SNR_V = \frac{\left[\frac{1}{\sqrt{2\pi}}\frac{v_n}{\sigma}\right]}{\sigma_V} \tag{68}$$

In terms of debiased and normalized correlator output quantities, this becomes

$$SNR_V = \sqrt{2N_t} \times \sqrt{C^2 + S^2} \tag{69}$$

where N_t, C, and S are defined by Eqs. (29), (30), and (31). Assuming that the stopped-tone signal-to-noise ratio is large, $SNR_V >> 1$, the phase variance (in radians^2) is

$$\sigma_\phi^2 = \frac{1}{SNR_V^2} = \frac{1}{2N_t[C^2 + S^2]} \tag{70}$$

VIII. Summary

We have reviewed phase calibration tone signal processing as implemented in the JPL Block II correlator. We have discussed the conventions that define the Block II correlator output in sufficient detail so that tone amplitudes, phases, and their respective variances may be calculated. Thomas's discussion of tone signal processing and tone variance for the Block 0 correlator [4] has been updated as it applies to the Block II correlator. The most important difference between the two correlators is that the Block II phase model has much finer quantization than does the Block 0. The chief result of our study is that, to within ≈10 percent accuracy, the tone amplitude variance is just a function of the number of bits per integration [Eqs. (42) and (65)], and the phase variance is just a function of the tone amplitude and the number of bits [Eq. (70)]. This result was based on assuming the following signal characteristics:

(1) The dominant noise on the signal is random white noise (Gaussian)

(2) Third-order intermodulation products are small $(v_n/\sigma)^2 << 1$

and the following signal-processing characteristics:

(1) Sampling: bandpass shape and sampling rate lead to a small autocorrelation

(2) DC bias of the 1-bit clipper is negligible

(3) Quantization effects of the correlator phase model are negligible

The size of these effects has been theoretically calculated and then confirmed with measurements of real VLBI data. For a typical Mk III VLBI experiment, the effects of phase model quantization and clipper bias are estimated to contribute less than 1 percent to the tone variance. The largest effect is from autocorrelation due to oversampling and imperfect (nonsquare) bandpass shape. This effect alters the tone variance by ±10 percent or less. It is expected that, for many applications, 10 percent accuracy will be sufficient.

Acknowledgments

Discussions with Ian Galton, Brooks Thomas, and Dave Fort helped to clarify the material presented in this article. Thanks go to Steve Lowe and Bob Treuhaft for providing comments on a draft of this article. This article is dedicated to Eleanor and Elaine Sanchez in recognition of their dedication to the pursuit of scholarly excellence.

References

[1] A. E. E. Rogers, *A Receiver Phase and Group Delay Calibrator for Use in Very Long Baseline Interferometry*, Haystack Observatory Technical Note 1975-6, Haystack Observatory, Westford, Massachusetts, 1975.

[2] A. E. E. Rogers, *Mk III Documentation*, Technical Manual TM 18915, Chapter 3, "Video Converter," Section 3.0, Haystack Observatory, Westford, Massachusetts, p. VC-8, item 3.0, January 1, 1982.

[3] J. B. Thomas, "The Tone Generator and Phase Calibration in VLBI Measurements," *The Deep Space Network Progress Report 42-44, January and February 1978*, Jet Propulsion Laboratory, Pasadena, California, pp. 63–74, April 15, 1978.

[4] J. B. Thomas, *An Analysis of Radio Interferometry With the Block 0 System*, JPL Publication 81-49, Jet Propulsion Laboratory, Pasadena, California, Appendix F, December 15, 1981.

[5] J. B. Thomas, *Interferometry Theory for the BlockII Processor*, JPL Publication 87-29, Jet Propulsion Laboratory, Pasadena, California, October 15, 1987.

[6] J. H. van Vleck and D. Middleton, "The Spectrum of Clipped Noise," *Proc. IEEE*, vol. 54, no. 1, 1966.

[7] C. S. Williams, *Designing Digital Filters*, Appendix C, Englewood Cliffs, New Jersey: Prentice-Hall, 1986.

Appendix A
Theoretical Digital Autocorrelation

This appendix presents digital autocorrelation as a function of integer bits of delay offset, τ, in Table A-1. The calculations have been done for three different bandpasses:

$n_p =$ 7 is the Mk III 7-pole Butterworth filter

$n_p =$ 11 is the Mk II 11-pole Butterworth filter

$n_p = \infty$ is a square bandpass filter

All three cases are evaluated using the same sample rate and the same filter cutoff frequency:

$\nu_s =$ 4.0 MHz is the sample rate

$\nu_0 =$ 1.8 MHz is the filter bandwidth (also known as the cutoff frequency)

Note how rapidly $\tilde{R}(\tau)$ approaches zero for both the 7- and 11-pole Butterworth filters. As a result, only $\pm$ a few bits contribute to the sum over $\tau \neq 0$ in the calculation of the tone variance, σ_V^2:

$$\sigma_V^2 = \frac{1}{2N_t}\left[1 + \sum_{\tau \neq 0} \tilde{R}(\tau)\right] \tag{A-1}$$

The resulting total contribution to σ_V^2 from $\tilde{R}(\tau)$ is $\leq \pm 10$ percent.

Figure A-1 plots the results presented in Table A-1. Note the normalization $\tilde{R}(\tau = 0) = 1$. All three cases represent different idealized bandpasses that are slightly oversampled. Note that the autocorrelation for the Mk II filter asymptotically approaches zero faster than it does for the square bandpass filter, and the Mk III approaches zero faster than does either the square or the Mk II filter.

Table A-1. Digital autocorrelation.

τ, bits	$\tilde{R}(\tau, n_p = 7)$	$\tilde{R}(\tau, n_p = 11)$	$\tilde{R}(\tau, n_p = \infty)$
0	$+1.0$	$+1.0$	$+1.0$
$\pm$ 1	$+9.58 \times 10^{-2}$	$+1.04 \times 10^{-1}$	$+1.09 \times 10^{-1}$
$\pm$ 2	-7.84×10^{-2}	-9.17×10^{-2}	-1.04×10^{-1}
$\pm$ 3	$+5.59 \times 10^{-2}$	$+7.48 \times 10^{-2}$	$+9.54 \times 10^{-2}$
$\pm$ 4	-3.48×10^{-2}	-5.62×10^{-2}	-8.41×10^{-2}
$\pm$ 5	$+1.89 \times 10^{-2}$	$+3.86 \times 10^{-2}$	$+7.07 \times 10^{-2}$
$\pm$ 6	-8.87×10^{-3}	-2.40×10^{-2}	-5.61×10^{-2}
$\pm$ 7	$+3.38 \times 10^{-3}$	$+1.31 \times 10^{-2}$	$+4.09 \times 10^{-2}$
$\pm$ 8	-8.17×10^{-4}	-5.84×10^{-3}	-2.60×10^{-2}
$\pm$ 9	-1.53×10^{-4}	$+1.49 \times 10^{-3}$	$+1.21 \times 10^{-2}$
$\pm$10	$+3.84 \times 10^{-4}$	$+7.37 \times 10^{-4}$	0
$\pm$11	-3.36×10^{-4}	-1.60×10^{-3}	-9.94×10^{-3}
$\pm$12	$+2.23 \times 10^{-4}$	$+1.68 \times 10^{-3}$	$+1.73 \times 10^{-2}$
$\pm$13	-1.25×10^{-4}	-1.40×10^{-3}	-2.20×10^{-2}
$\pm$14	$+5.98 \times 10^{-5}$	$+1.02 \times 10^{-3}$	$+2.40 \times 10^{-2}$
$\pm$15	-2.37×10^{-5}	-6.53×10^{-4}	-2.36×10^{-2}
$\pm$16	$+6.42 \times 10^{-6}$	$+3.67 \times 10^{-4}$	$+2.10 \times 10^{-2}$
$\pm$17	$+3.85 \times 10^{-7}$	-1.71×10^{-4}	-1.68×10^{-2}
$\pm$18	-2.21×10^{-6}	$+5.10 \times 10^{-5}$	$+1.16 \times 10^{-2}$
$\pm$19	$+2.07 \times 10^{-6}$	$+1.22 \times 10^{-5}$	-5.75×10^{-3}
$\pm$20	-1.42×10^{-6}	-3.82×10^{-5}	0

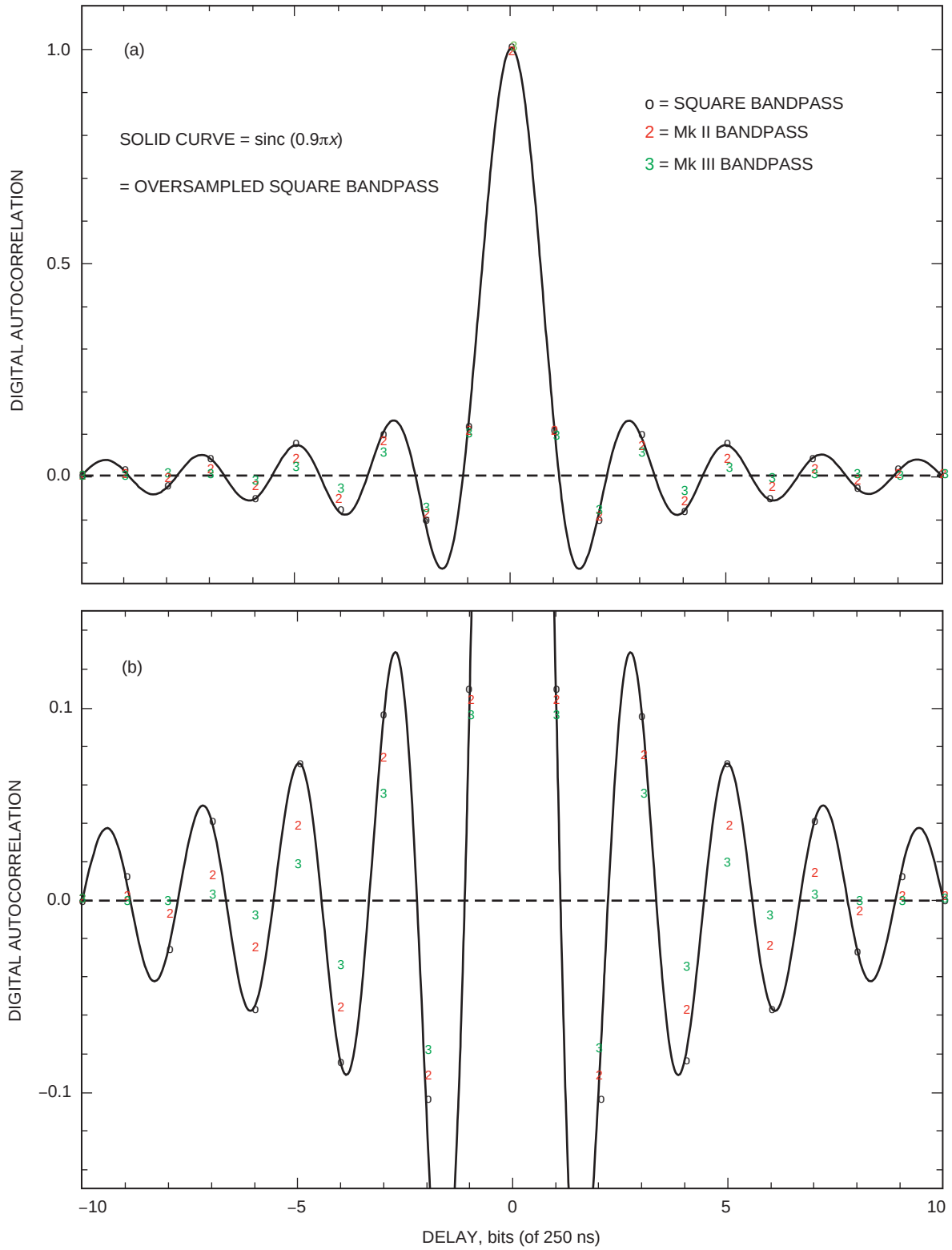

Fig. A-1. Digital autocorrelation for an oversampled bandpass. The bandpass cutoff frequency is 1.8 MHz; the sample rate is 4 Mbit/s: (a) the solid curve is for an ideal square bandpass with "o" marking the values at integer bits of delay and "2" and "3" marking values for ideal 11- and 7-pole Butterworth filters, respectively, and (b) an expanded view of Fig. A-1(a) in order to clearly show the differences between the three filters considered.

Appendix B
Mk II Measured Autocorrelation

Digital autocorrelation as a function of integer bits of delay offset, τ, has been both theoretically calculated and measured for a nominal Mk II configuration in Table B-1. The calculations have been done for the theoretical Mk II bandpass using the following parameters:

n_p= 11, i.e., an 11-pole Butterworth filter

ν_0= 1.8 MHz, the Butterworth cutoff frequency

ν_s= 4.0 MHz, a sampling rate slightly above the Nyquist rate

The measured values come from Mk II experiment 90ss351 (December 17, 1990, DSS 65 to DSS 63, scan 3, channel 5) as processed with the Block II correlator (cf., [5]) and extracted with Tom Lockhart's CDUMP utility program[10] (CDUMP lags 8 to 16 correspond to $\tau = 0$ to $\tau = 8$).

The results for $\tau = 0$ bits do not depend upon the bandpass shape, but they do reflect the scaling factors used in Block II processing. Thus, the measured results confirm our assumptions regarding scaling. The measured autocorrelation from DSS 65 agrees qualitatively and to some extent quantitatively with the theory. In particular, we note the alternation of signs when going from $\tilde{R}(\tau = 1)$ to $\tilde{R}(\tau = 2)$ to $\tilde{R}(\tau = 3)\ldots$ to $\tilde{R}(\tau = 7)$. However, the results from DSS 63 have poor agreement with the theory. Indeed, transforming the time domain autocorrelation results to the frequency domain showed that the DSS-63 bandpass was a very poor approximation of a Butterworth filter. The amplitude response of a Butterworth filter is fairly flat until very near the cutoff frequency, after which the amplitude decreases rapidly. In contrast, the DSS-63 filter amplitude response increased by ≈3 dB in power going from 0.1 to 0.35 MHz and then decreased by ≈3 dB going from 0.35 to 1.7 MHz. The anomalous frequency response at DSS 63 was confirmed by Jose A. Perea.[11]

Table B-1. Mk II theoretical versus measured autocorrelation.

τ, bits	$\tilde{R}(\tau, n_p = 11)$	$\tilde{R}(\tau, \text{DSS 65})$	$\tilde{R}(\tau, \text{DSS 63})$
0	+1.0	+1.0	+1.0
1	+0.104	+0.145	−0.135
2	−0.092	−0.026	−0.153
3	+0.075	+0.058	+0.056
4	−0.056	−0.015	−0.079
5	+0.039	+0.036	+0.053
6	−0.024	−0.007	−0.041
7	+0.013	+0.022	+0.034
8	−0.006	+0.006	+0.007

[10] T. G. Lockhart, Tracking and Applications Section, Jet Propulsion Laboratory, Pasadena, California, September 21, 1988.

[11] J. A. Perea, JPL teletype message to P. Wolken (internal document), Jet Propulsion Laboratory, Pasadena, California, January 31, 1991.

Appendix C
Mk III Measured Autocorrelation

Digital autocorrelation as a function of integer bits of delay offset, τ, has been both theoretically calculated and experimentally measured for a nominal Mk III configuration in Table C-1. The calculations have been done for the theoretical Mk III 7-pole Butterworth bandpass filter using the following parameters:

$n_p =$ 7, i.e., a 7-pole Butterworth filter

$\nu_0 =$ 1.8 MHz, the Butterworth cutoff frequency

$\nu_s =$ 4.0 MHz, a sample rate slightly higher than the Nyquist rate

The measured values come from Mk III experiment 90cs316 (November 12 , 1990, DSS 15 to DSS 65, scan 26, channel 1) as processed with the Block II correlator (cf., [5]) and extracted with Tom Lockhart's CDUMP utility program[12] (CDUMP lags 8 to 16 correspond to $\tau = 0$ to $\tau = 8$).

The results for $\tau = 0$ bits do not depend upon the bandpass shape, but they do reflect the scaling factors used in Block II processing. Thus, the measured results confirm our assumptions regarding scaling for the autocorrelation at zero delay, $\tilde{R}(\tau = 0) = 1$. The measured autocorrelations agree qualitatively and to some extent quantitatively with the theory. In particular, we note the alternation of signs when τ is increased/decreased by a bit. Also, we note the symmetry of the measured autocorrelation as evidenced by the agreement of $\tilde{R}(\tau)$ with $\tilde{R}(-\tau)$.

There do appear to be some systematic problems though. While the $\tilde{R}(\tau)$ for a given channel repeats rather well from scan to scan, there are systematic differences amongst the $\tilde{R}(\tau)$'s for various channels. For example, $\tilde{R}(\tau = 1$ bit) repeats between scans 26 and 27 to $\approx\pm 0.001$ (with an outlier differing by 0.01), whereas channel-to-channel agreement is $\approx\pm 0.025$. Also, the $\tilde{R}$'s for $\tau \neq 0$ are smaller than predicted by roughly a factor of ≈ 2, which can be partially accounted for by increasing ν_0 by ≈ 5 percent to ≈ 1.89 MHz. The channel-to-channel variations also may be due to variations in a particular channel's filter cutoff frequency, ν_0.

Table C-1. Mk III theoretical versus measured autocorrelation.

τ, bits	$\tilde{R}(\tau, n_p = 7)$	$\tilde{R}(\tau, \text{DSS 15})$	$\tilde{R}(\tau, \text{DSS 65})$
0	+1.0	+1.0	+1.0
+1	+0.095	+0.049	+0.054
−1	+0.095	+0.047	+0.052
+2	−0.078	−0.043	−0.050
−2	−0.078	−0.044	−0.051
+3	+0.056	+0.031	+0.032
−3	+0.056	+0.030	+0.031
+4	−0.035	−0.018	−0.024
−4	−0.035	−0.020	−0.026
+5	+0.019	+0.011	+0.013
−5	+0.019	+0.010	+0.012
+6	−0.0089	−0.0043	−0.0060
−6	−0.0089	−0.0057	−0.0074
+7	+0.0034	+0.0033	+0.0005
−7	+0.0034	+0.0018	−0.0009

[12] T. Lockhart, op. cit.

Appendix D
Side-band Rejection

We have assumed in this article that the effect of finite side-band rejection is negligible. In this appendix, we briefly examine that assumption. Define side-band rejection, $r(\nu)$, at frequency, ν, and with bandpass power response, $A(\nu)$, to be

$$r(\nu) = \frac{A(\nu)}{A(-\nu)} \tag{D-1}$$

For our purposes, it is convenient to reformulate the above expression in units of dB and as a function of the voltage response, $V(\nu) = \sqrt{A(\nu)}$:

$$r(\nu) = 20 \log \left[\frac{V(+\nu)}{V(-\nu)} \right] \text{ (dB)} \tag{D-2}$$

To the extent that side-band rejection is a constant, the Fourier transform of $A(\nu)$ and the normalization both will be scaled by the same factor, resulting in no net change in the autocorrelation, $R(\tau)$. There may be a small effect due to the change of $r(\nu)$ with frequency. We will neglect this and assume that the single side-band converter has constant side-band rejection as a function of frequency. Thus, integrals of $A(\nu)$ over ν [e.g., Eq. (52)] can be taken from zero to $+\infty$ instead of over $\pm\infty$.

Table D-1 presents measured values of side-band rejection. The Block II correlator was used to extract eight phase calibration tones at approximate baseband frequencies of ± 0.25, ± 0.75, ± 1.25, and ± 1.75 MHz (actual frequencies were slightly offset by 0.01 to 0.02 MHz, e.g., $+0.24$ and -0.26 MHz). The upper- and lower-side-band tone voltages, $V(+\nu)$ and $V(-\nu)$, at baseband frequencies $\pm\nu$ were used to obtain $r(\nu)$ according to Eq. (D-2). The data used to estimate $r(\nu)$ are from experiment 90ca100 (DSS 15 and DSS 45, April 1990, scan 144). By comparing with $r(\nu)$'s estimated from scan 143, we estimate realistic uncertainties on the values of $r(\nu)$ are $\approx \pm 0.5$ dB exclusive of long term (>1000-s) systematic errors.

The Mk III video converter nominal specification [2] is that side-band rejection should be more than 20 dB for baseband frequencies of 1 kHz to 8 MHz (with video converter local oscillator frequencies anywhere in the range of 100 to 500 MHz). Notice that none of the 28 video converters has an r (1.74 MHz) that meets the specification of -20 dB.

The video converters could have been retrofitted with new single side-band converters in an attempt to meet the specification. However, S. DiNardo[13] estimated retrofitting costs would have been a substantial fraction of the cost of the entire video converter. The retrofit was not done before the Mk III system was replaced with the Mk IV system. The Mk IV system has not yet been tested by the author for side-band rejection.

[13] S. DiNardo, private communication, Tracking and Applications Section, Jet Propulsion Laboratory, Pasadena, California, January 1991.

Table D-1. Measured Mk III side-band rejection versus baseband frequency.

Channel	r(0.25 MHz)	r(0.75 MHz)	r(1.25 MHz)	r(1.75 MHz)
		DSS 15		
1	−23.5	−20.7	−18.0[a]	−16.1[a]
2	−22.4	−24.4	−21.7	−13.4[a]
3	−22.4	−21.4	−17.8[a]	−13.6[a]
4	−26.5	−28.9	−19.9[a]	−12.2[a]
5	−28.2	−22.2	−17.9[a]	−8.7[a]
6	−21.3	−30.2	−25.9	−13.1[a]
7	−28.8	−25.7	−21.2	−11.3[a]
8	−21.6	−25.1	−20.3	−12.1[a]
9	−21.7	−29.3	−24.9	−13.3[a]
10	−21.1	−17.5[a]	−12.1[a]	−8.9[a]
11	−20.9	−33.0	−27.5	−12.8[a]
12	−28.5	−26.2	−18.7[a]	−10.5[a]
13	−18.4[a]	−26.0	−25.3	−14.5[a]
14	−25.9	−25.6	−21.0	−10.9[a]
		DSS 45		
1	−27.8	−32.5	−28.9	−11.6[a]
2	−27.7	−25.1	−28.2	−11.6[a]
3	−20.3	−31.9	−29.5	−12.0[a]
4	−27.0	−19.6[a]	−21.4	−12.8[a]
5	−28.5	−19.6[a]	−23.0	−11.6[a]
6	−21.6	−34.5	−28.4	−13.1[a]
7	−26.3	−29.2	−28.3	−13.9[a]
8	−35.3	−23.2	−23.4	−15.0[a]
9	−26.0	−23.8	−27.3	−13.3[a]
10	−26.7	−24.6	−27.8	−13.7[a]
11	−28.1	−25.8	−25.5	−14.3[a]
12	−22.0	−33.7	−28.8	−11.5[a]
13	−23.3	−31.0	−29.1	−12.9[a]
14	−22.3	−32.5	−31.3	−12.6[a]

[a] Fails to meet the −20 dB specification for side-band rejection.